Exploiting VERITAS Timing Information
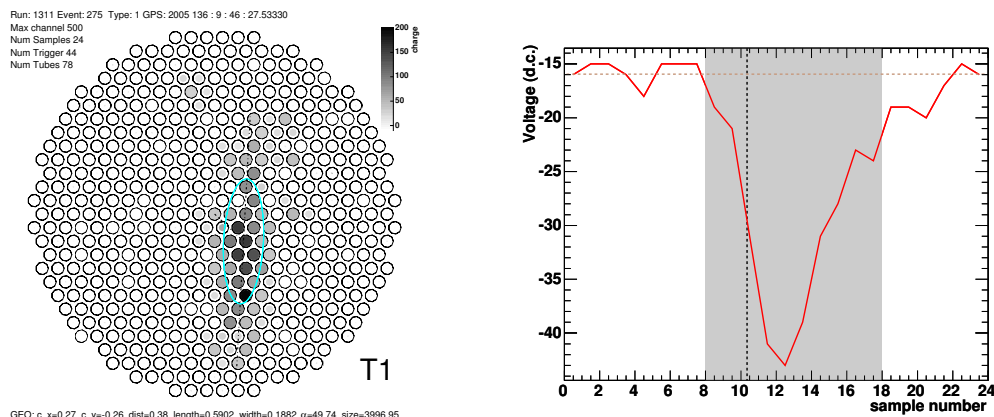
J. Holder for the VERITAS Collaboration
School of Physics and Astronomy, University of Leeds, U.K.
Presenter: J. Holder (jh@ast.leeds.ac.uk), uki-holder-J-abs2-og27-poster

The 499 pixel photomultiplier cameras of the VERITAS gamma ray telescopes are instrumented with 500MHz sampling Flash ADCs. This paper describes a preliminary investigation of the best methods by which to exploit this information so as to optimize the signal-to-noise ratio for the detection of Cherenkov light pulses. The FADCs also provide unprecedented resolution for the study of the timing characteristics of Cherenkov images of cosmic-ray and gamma-ray air showers. This capability is discussed, together with the implications for gamma-hadron separation.

1. Introduction

Imaging atmospheric Cherenkov telescopes use large mirror areas to reflect the Cherenkov photons from cosmic-ray and gamma-ray air showers onto a photo-detector camera, usually comprised of photo-multiplier tubes (PMTs). The number of photoelectrons generated at each PMT is directly proportional to the charge under the PMT output pulse, and this is easily measured using ADCs with fixed-length integration gates. An alternative method is to use "Flash" ADCs to rapidly sample the output pulse and record the complete pulse shape. This allows to maximize the signal-to-noise ratio for individual pulses at the analysis stage, lowering the effective energy threshold of the telescope [1]. A number of authors have suggested that the timing and pulse shape information could also be used to improve sensitivity through improved gamma-hadron separation or better reconstruction of shower parameters (core location, primary energy, etc.) [2, 3].


Figure 1. Left: The charge distribution across the camera for a cosmic-ray event (the grey scale is in d.c.). **Right:** The FADC trace for a PMT in the image. The dashed vertical line indicates T_0 for this pulse.

The VERITAS collaboration have been operating the first of four 12 m aperture telescopes at the Mt Hopkins basecamp (altitude=1275 m) since January 2005 [4]. The 499 pixel camera is instrumented with 500 MHz sampling FADCs with a memory depth of 32μs and a dynamic range of 8 bits [1]. The deep memory simplifies array operation and will allow us to read out all telescopes when the array is triggered, including those which do not generate a local trigger themselves. Typically, the readout window is 24 samples (48 ns) per PMT.

Figure 1 shows a typical event with a FADC trace. At the FADCs, the PMT signal pulse for an input delta function has a risetime (10% to 90%) of 3.3 ns and a width of 6.5 ns.

2. Timing calibration

Before any analysis which uses the pulse timing information can be considered, the PMT camera timing response must be calibrated. The first stage of this is to correct for the fixed transit time differences between channels, mainly caused by the non-uniform high voltages applied to the PMTs. A laser is used to produce a brief (~ 4 ns) light pulse which is sent via fibre-optic cable to a diffuser situated in front of the PMT camera. At the camera face, the light flash is uniform in intensity and arrival time. The pulse arrival time at each PMT, T_0, is defined as the half-height point on the pulse leading edge. The mean value of T_0 for a single channel, measured relative to the mean pulse arrival time over all channels, is the fixed time offset for that channel. This is subtracted from the measured pulse arrival time in each channel for each event in order to flat-field the time response over the camera. Figure 2 shows these mean values for all channels as a function of the PMT high voltage. We note that the FADC boards contain a 6 ns programmable delay which is used to compensate for these transit time offsets at the trigger level to a resolution of 0.85 ns.
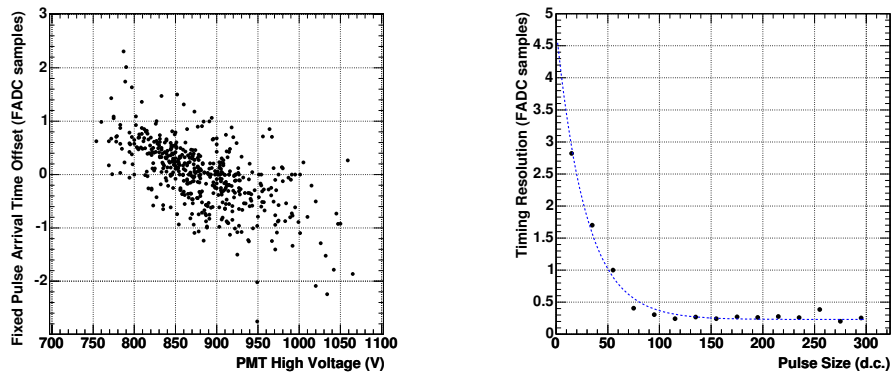
Figure 2. Left: The mean fixed time offset per channel plotted against the high voltage for each PMT. **Right:** The pulse timing resolution as a function of the integrated charge in the pulse. The dashed line is described in the text.

The timing resolution, T_{res}, for the pulse arrival times is also important and depends on the pulse time reconstruction method, the pulse size and the night-sky background level. The VERITAS FADCs are housed in four VME crates; while the timing between FADCs in the same crates is synchronised, there is a crate-to-crate jitter of ~ 1 FADC sample (2 ns) which adversely affects the timing resolution. To correct for this, one FADC channel in each crate receives a copy of the telescope trigger signal. This acts as a fixed time reference for each crate which can be used to correct the crate-to-crate jitter on an event-by-event-basis. Figure 2 shows the time resolution for one channel as a function of laser pulse size. The empirically derived function shown is $T_{res} = 13 \exp^{-0.035*(size+30)} + T_{res0}$, where $size$ is the integrated charge in the pulse and T_{res0} is the timing resolution for large pulses, typically a few 100 picoseconds.

3. Gamma-Hadron Separation

The longitudinal development of an air shower is reflected in the long axis of the elliptical image recorded in the camera. The photon arrival time profile along this axis is largely a result of geometrical path length

differences, and hence the shower core distance. As the shower particles move faster than the speed of light in air, when the shower has a small core distance Cherenkov light emitted from lower in the atmosphere is received at the telescope first. At large core distances, this situation is reversed, as the Cherenkov light travel time from the shower to the telescope dominates. The effect of this is to produce a timing gradient along the long axis of the image, the size and sign of which depend upon the core distance. For gamma-ray showers from a point source at the centre of the field of view, the shower core distance is directly related to the angular $distance$ in the camera of the image from the source position.

Figure 3 shows the pulse arrival time as a function of PMT position along the long axis of the image for the cosmic-ray event shown in figure 1. The gradient of a straight line fit to this graph is $Tgrad_x$. Also shown in figure 3 is the correlation between $distance$ and $Tgrad_x$ for simulated and real gamma-ray showers. The real data is a combination of high elevation observations of the Crab Nebula and Markarian 421 with the first VERITAS telescope. Background cosmic-ray images (and in particular short arcs generated by local muons) which survive the usual gamma-ray cuts have a flat distribution of $Tgrad_x$, with a mean value of $Tgrad_x \sim 0$ regardless of the image $distance$. This implies that it may be possible to use the image timing gradient as an additional gamma-hadron discriminant. We do this by fitting a line to the data points in figure 3 and then selecting a gamma-ray region defined by an upper and lower bound parallel to this line. The dashed lines in the figure show the gamma-ray selection region which provides the most improvement to the significance; however this improvement is only 5%.
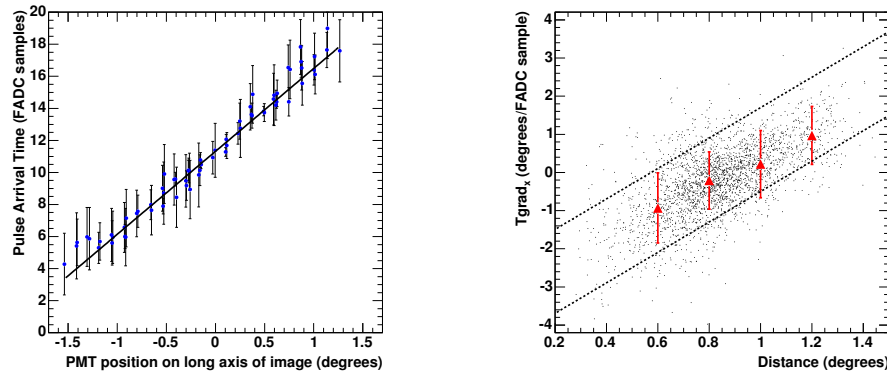
Figure 3. Left: The Cherenkov pulse arrival time distribution (in units of FADC samples = 2 ns) along the long axis of the image in figure 1. **Right:** $Tgrad_x$ as a function of $distance$ for real (large triangles) and simulated (small points) gamma-ray showers. Dashed lines show the optimum gamma-ray selection region.
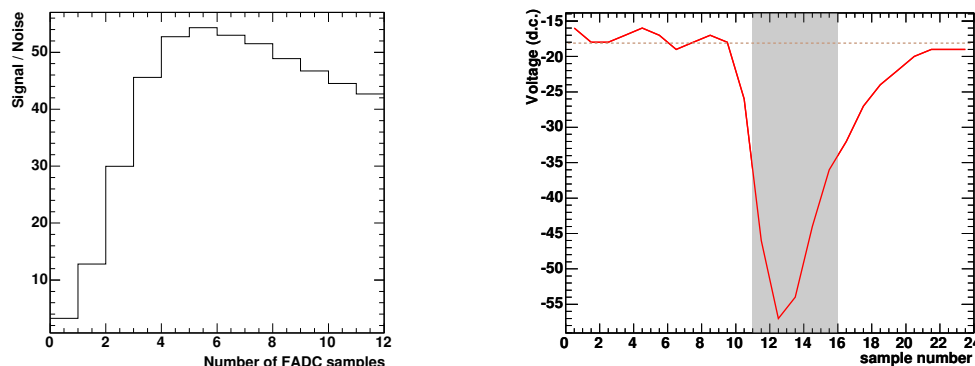
4. Improving the Signal-to-Noise

Having detailed pulse shape information also allows us to optimize the accuracy of the charge measurement by application of signal processing algorithms. We describe one such method here; various other techniques (matched filters [1], pulse shape fitting, etc.) are also under investigation.

The simplest way to improve the signal-to-noise ratio on the charge measurement is to reduce the size of the FADC integration window; however, care must be taken that the reduced window is correctly located around the pulse position. We achieve this by a two-pass method: first, the images are parameterized using a fixed, wide (20 ns) integration gate and $Tgrad_x$ is measured, then the $Tgrad_x$ value is used to define the start position of a shortened integration gate which will be different for each PMT channel. The images are then

re-parameterized using the shortened gate and the parameters written out for use in the gamma-ray selection analysis. The optimum size of the shortened gate is determined to be 5 FADC samples (10 ns) by measuring the ratio of the integrated PMT signal pulse and the night sky background noise as a function of the integration window size (see figure 4).

The benefit of the two-pass method is not simple to quantify, as other parameters in the analysis also require optimization (e.g. image cleaning thresholds, image parameter cut positions), and the best values of these parameters will be different for the two-pass method and a simple fixed integration gate method; however the results of applying optimizing image parameter cuts to a 3.9 hour Crab Nebula data set indicate an improvement to the final significance of 10%. Perhaps more importantly, this method is relatively robust against long-term drifts in the trigger time which affect the average pulse position in the FADC window.

Figure 4. Left: The signal-to-noise ratio as a function of the integration window size (in FADC samples) **Right:** The FADC trace for a PMT with the shaded window indicating the shortened integration gate placed according to the image's $T\,grad_x$ value.

5.   Conclusion

A preliminary examination of the timing information provided by the VERITAS FADCs verifies that the effective charge integration gate can be reduced to 10 ns. While the muon background currently limits the analysis threshold of the first VERITAS telescope, the reduced charge integration gate should result in a correspondingly reduced energy threshold for analysis when stereo data becomes available. This preliminary study does not indicate a significant improvement in gamma-hadron separation using the timing information; however, this situation may also change when the muon background is removed. Refinements to the simulations, the application of advanced digital signal processing methods and an increased dataset of gamma-ray source observations should all help future studies in this area.

References

[1] J. H. Buckley et al., 28th ICRC, Tsukuba (2003)
[2] M.D. Roberts et al., J. Phys. G. 24, 255 (1998)
[3] M. Hess et al., Astropart. Phys. 11, 363 (1999)
[4] J. Holder et al., 29th ICRC, Pune (2005)